

## Lattice-based Monte Carlo method for telechelic chain molecules

Behnaz Bozorgui and Daan Frenkel

*FOM Institute for Atomic and Molecular Physics, Kruislaan 407, 1098 SJ Amsterdam, The Netherlands*

(Received 31 October 2006; published 26 March 2007)

We present a Monte Carlo (MC) scheme that makes it possible to perform efficient simulations of dense systems of self-avoiding polymers on a lattice. We show that the method is particularly useful to simulate dense systems of polymers with functionalized end groups. We compare the efficiency of the scheme with the configurational bias MC method and indicate the regime where the present approach is the method of choice.

DOI: [10.1103/PhysRevE.75.036708](https://doi.org/10.1103/PhysRevE.75.036708)

PACS number(s): 05.10.Ln, 82.20.Wt, 82.35.Gh

### I. INTRODUCTION

Polymer simulations are often time consuming because the natural dynamics of polymers is slow. For this reason, many Monte Carlo methods have been developed that sample the configurational space of polymeric systems by carrying out efficient “unphysical” trial moves, i.e., moves that do not correspond to the slow natural motion of polymeric chains, yet do preserve the Boltzmann distribution (see, e.g., reptation [1,2], pivot moves [3], configurational biased Monte-Carlo (CBMC) methods [4], connectivity-altering moves [5], hyperparallel tempering [6], wormhole moves [7].) In spite of the great variety in computational schemes, there are situations where polymer simulations are still very inefficient. This is particularly true in the case of polymers that can bind to heterogeneous surfaces. It is, for instance, time consuming to compute the free energy of a system of polymers that can either be nonadsorbing or form bridges and loops between surfaces.

Below, we describe a grand-canonical Monte Carlo technique that is particularly efficient for simulations of polymers that interact strongly with surfaces. The basic idea is to use the statistics of non-self-avoiding walks to grow self-avoiding walks (SAWs) on a lattice. While there exists no “cheap” method to enumerate the number of SAW chain conformations in a given system, efficient algorithms exist to count the number of polymer conformations that correspond to ideal and nonreversible (NR) random walks. NR walks are random walks that exclude 180° reversal: i.e., retracing the last step is excluded. We can count the number of NR walks using the so-called moment-propagation (MP) scheme [8]. To be more precise, during a trial move we enumerate all NR walks for one polymer, while keeping the positions of all other polymers fixed. The exact enumeration of NR walks implies that if there is only a single acceptable conformation for the additional polymer, it will be included in the enumeration. However, some acceptable NR configurations may not be self-avoiding and will therefore be rejected at a later stage.

This prescreening of acceptable configurations greatly enhances the success rate of particle-insertion moves. In fact, as we will show, the present method becomes much more efficient than the CBMC method at high densities. Below, we explain how we can incorporate the number of NR walks in a lattice-based CBMC scheme and use this scheme to grow self-avoiding chains. We will demonstrate that the MC ac-

ceptance rule satisfies detailed balance. Finally, we show a number of results for nonadsorbing and for telechelic chains, on the one hand to validate the present method and, on the other, to quantify its relative performance with respect to other existing schemes.

### II. METHOD

Consider a regular lattice with coordination number  $z$ . We assign a set of  $z$  numbers to each lattice site. Each number represents a weight that is related to one of the neighbors. Let  $i$  and  $j$  be two neighboring sites on the lattice.  $\omega'(i; j \rightarrow i; l)$  is defined as the Boltzmann-weighted number of nonreversible walks of length  $l$ , which end at site  $i$  along the bond  $j \rightarrow i$ . Hence  $\omega'(i; j \rightarrow i; l)$  can be viewed as the partition sum of a single NR chain that has its end segment along the link  $i-j$ . As NR walks cannot retrace their last step, it is necessary to label not simply the number of walks arriving at site  $i$ , but also the lattice site last visited. For instance, if we wish to calculate  $\omega'(i; j \rightarrow i; l+1)$  knowing the corresponding weights for walks of length  $l$  we should exclude those walks that went from  $i$  to  $j$  in the previous step

$$\omega'(i, j \rightarrow i; l+1) = \left( \sum_{j' \in \langle j \rangle'} \omega'(j, j' \rightarrow j; l) \right) \omega(i, 0), \quad (1)$$

in which  $\langle j \rangle$  is defined as the set of  $z$  nearest neighbors of site  $j$ , and by  $\langle j \rangle'$  we mean the conformation-dependent set which excludes the last step (site  $i$  in the above case).  $\omega(i, 0)$  is defined as the Boltzmann weight due to the interaction of a monomer at site  $i$  with other polymers or with external interactions, such as walls. This Boltzmann weight is a measure of the accessibility of site  $i$  for a monomeric unit (chain of length 0). As an example, for hard monomers,  $\omega(i, 0) = 0$  when the site is occupied and 1 when it is empty. It is then sufficient to know  $\omega(i, 0)$  for all lattice sites  $i$  to calculate all the weights for any length.

The weights  $\omega'$  determine the likelihood of growing a nonreversible walk with a fixed length  $l$  coming from a specified direction. Using these weights in the insertion algorithm will introduce a bias that facilitates the finding of acceptable conformations for the polymer to be inserted. It would, of course, have been possible (in fact, easier) to calculate the number of ideal random walks and their corresponding weights. However, as very few ideal walks are completely NR, the subsequent step in the algorithm would

reject most of the walks thus generated, because at some points, they retrace their steps. For this reason, the use of NR weights is more efficient.

*Insertion algorithm.* Having computed all weights  $\omega'(i_1, j \rightarrow i_1; n)$  for  $n=0, 1, \dots, l$ , we can now start inserting the self-avoiding chain, using these weights as a bias. Lattice sites from which there emerge large numbers of NR walks will be favored over those that spawn none, or only few. In what follows, we will assume that nonbonded monomers of the same chain cannot occupy the same lattice site, but do not interact otherwise. If that is the case, self-avoidance effects only come into play upon growing the 4th polymer segment (at least, on a simple cubic lattice). However, it is straightforward to generalize the present approach to the case where intrachain interactions are longer ranged. We will also assume that all the polymers are of the same length. We generate a trial conformation of a chain with fixed length  $l$  following these steps:

(1) The first monomer  $i_1$  is selected with probability

$$p_1 = \frac{\sum_{j \in \langle i_1 \rangle} \omega'(i_1, j \rightarrow i_1; l)}{Q_{eff}}.$$

The sum in the numerator is a sum over all  $z$  neighbors of site  $i_1$  and it gives the total number of nonreversible walks of length  $l$  terminating at site  $i_1$  from different directions.  $Q_{eff}$  is the total number of NR walks of length  $l$  in the system of  $M$  lattice sites:

$$Q_{eff} = \sum_{i=1}^M \sum_{j \in \langle i \rangle} \omega'(i, j \rightarrow i; l). \quad (2)$$

The above expression simplifies to  $Mz(z-1)^{l-1}$  for an empty lattice containing  $M$  sites.

(2) The second monomer is selected from one of the  $z$  neighbors of  $i_1$ , called  $i_2$ , with a probability

$$p_2 = \frac{\omega'(i_1, i_2 \rightarrow i_1; l)}{\sum_{j \in \langle i_1 \rangle} \omega'(i_1, j \rightarrow i_1; l)}.$$

(3) The third monomer is selected from one of the neighbors of  $i_2$  with probability

$$p_3 = \frac{\omega'(i_2, i_3 \rightarrow i_2; l-1)}{\sum_{j \in \langle i_2 \rangle'} \omega'(i_2, j \rightarrow i_2; l-1)}.$$

(4) The fourth monomer is selected from one of the neighbors of  $i_3$  with probability

$$p_4 = \frac{\omega'(i_3, i_4 \rightarrow i_3; l-2)}{\sum_{j \in \langle i_3 \rangle'} \omega'(i_3, j \rightarrow i_3; l-2)}.$$

(5) Starting with the fifth monomer we have to take into account the self-avoidance. The fifth monomer is chosen with the following probability:

$$p_5 = \frac{\omega'(i_4, i_5 \rightarrow i_4; l-3) \exp[-\beta u_{int}(i_5)]}{\sum_{j \in \langle i_4 \rangle'} \omega'(i_4, j \rightarrow i_4; l-3) \exp[-\beta u_{int}(j)]}.$$

The “internal” energy  $u_{int}(i_s)$  accounts for the interactions with all monomers 1 to  $s-1$ , that have been already grown.

(6) Step 5 is repeated until the whole chain is grown (unless the growth process terminated in a dead end, due to intrachain interactions). The probability of choosing the  $s$ th monomer equals to

$$p_s = \frac{\omega'(i_{s-1}, i_s \rightarrow i_{s-1}, l+2-s) \exp[-\beta u_{int}(i_s)]}{\sum_{j \in \langle i_{s-1} \rangle'} \omega'(i_{s-1}, j \rightarrow i_{s-1}, l+2-s) \exp[-\beta u_{int}(j)]}.$$

Once we have grown the whole chain, the move is accepted with the following probability:

$$\text{acc}(n_p \rightarrow n_p + 1) = \min \left\{ 1, \frac{\exp(\beta\mu) Q_{eff} \prod_{l=1}^N \langle \exp[-\beta u_{int}(i_l)] \rangle}{n_p + 1} \right\}. \quad (3)$$

The terms in angular brackets denote the weighted averages of Boltzmann factors of the internal potential along the chain, defined as

$$\langle \exp[-\beta u_s(i_s)] \rangle = \frac{\sum_{j \in \langle i_{s-1} \rangle'} \omega'(i_2, j \rightarrow i_2, l+2-s) \exp[-\beta u_{int}(j)]}{\sum_{j \in \langle i_{s-1} \rangle'} \omega'(i_2, j \rightarrow i_2, l+2-s)}. \quad (4)$$

To clarify the meaning of the acceptance rule, we decompose it into three different parts. The first part,  $\exp(\beta\mu)/(n_p+1)$  comes from the chemical potential or, equivalently, the average polymer density in the “osmotic reservoir” in contact with the system. We know this part before growing a chain or calculating any weight. The second part is  $Q_{eff}$  which comes from the NR guiding weights. To know this part we have to calculate NR weights before each trial of exchanging a new chain. However this part does not depend on the specific configuration that we grow. The only part in the acceptance argument that depends on the configurations is the product term. If we had ignored self-avoidance affects in the NR chain, the terms in Eq. (4) would have been equal to unity and the acceptance probability would have been determined only by  $Q_{eff}$ .

The main difference between the new biased scheme and CBMC is the presence of non-local guiding weights  $\omega'$ . In general, in a CBMC scheme a trial conformation will be generated using local conformation-dependent weights. In our scheme these weights carry long range information about acceptable conformations of the whole system. This facilitates the growing process and will increase the acceptance rate. In the next section, we show that the proposed algorithm satisfies detailed balance.

Now consider the situation in which a chain is randomly selected to be completely removed. First, we remove the chain and recalculate the guiding weights  $\omega'$ . Then we reconstruct the same old configuration monomer by monomer. At each step we calculate the weighted average of  $u_{int}$  which is defined in equation (4). After the whole chain has been retraced we will remove it with the probability:

$$\text{acc}(n_p + 1 \rightarrow n_p) = \min \left\{ 1, \frac{n_p \exp[-\beta\mu]}{Q_{eff} \prod_{l=1}^l \langle \exp[-\beta u_{int}(i_l)] \rangle} \right\}. \quad (5)$$

We considered several ways of improving upon the above algorithm. Since we know some parts of the acceptance argument before trying to grow a configuration, we could split the rejection criterion in two or three parts. This might increase the computational efficiency as we can reject a “doomed” trial configuration at an early stage. However, it turns out that splitting the acceptance procedure in parts is

not helpful for dense systems—and it is precisely for these systems that the present approach is most competitive. For this reason, we used the acceptance rule in the form given in Eqs. (3) and Eq. (5).

### III. DETAILED BALANCE

The acceptance rule in Eq. (5) should satisfy detailed balance (DB). Let us define  $\alpha(n_p \rightarrow n_p + 1)$  as the probability of generating a new configuration, and  $\text{acc}(n_p \rightarrow n_p + 1)$  as the probability of accepting it and let  $\alpha(n_p + 1 \rightarrow n_p)$  and  $\text{acc}(n_p + 1 \rightarrow n_p)$  denote the corresponding quantities for the reverse move. DB implies that

$$\frac{P_B(n_p) \alpha(n_p \rightarrow n_p + 1)}{P_B(n_{p+1}) \alpha(n_p + 1 \rightarrow n_p)} = \frac{\text{acc}(n_p + 1 \rightarrow n_p)}{\text{acc}(n_p \rightarrow n_p + 1)}, \quad (6)$$

where  $P_B(n_p)$  [ $P_B(n_{p+1})$ ] denotes the Boltzmann weight of the configuration with  $n_p$  ( $n_{p+1}$ ) polymers. Looking back at the insertion algorithm we can derive  $\alpha(n_p \rightarrow n_p + 1)$  by calculating the probability of the new configuration.

$$\begin{aligned} \alpha(n_p \rightarrow n_p + 1) &= \prod_{s=1}^l p_s = \frac{\sum_{j \in \langle i_1 \rangle} \omega'(i_1, j \rightarrow i_1; l)}{Q_{eff}} \frac{\omega'(i_1, i_2 \rightarrow i_1; l) \exp[-\beta u_{int}(i_2)]}{\sum_{j \in \langle i_1 \rangle} \omega'(i_1, j \rightarrow i_1; l) \exp[-\beta u_{int}(j)]} \frac{\omega'(i_2, i_3 \rightarrow i_2, l-1) \exp[-\beta u_{int}(i_3)]}{\sum_{j \in \langle i_2 \rangle'} \omega'(i_2, j \rightarrow i_2, l-1) \exp[-\beta u_{int}(j)]} \\ &\times \frac{\omega'(i_{s-1}, i_s \rightarrow i_{s-1}; l+2-s) \exp[-\beta u_{int}(i_s)]}{\sum_{j \in \langle i_{s-1} \rangle'} \omega'(i_{s-1}, j \rightarrow i_{s-1}; l+2-s) \exp[-\beta u_{int}(j)]} \dots \end{aligned}$$

We can rewrite the above equation in a simple form using Eqs. (1) and (4):

$$\alpha(n_p \rightarrow n_p + 1) = \frac{\exp(-\beta U_{int})}{Q_{eff} \prod_{s=1}^{l+1} \langle \exp[-\beta u_{int}(i_s)] \rangle},$$

where  $U_{int} = \sum_s u_{int}(i_s)$  denotes the total internal energy of the chain. By inserting  $\alpha(n_p \rightarrow n_p + 1)$  in Eq. (6) we recover the acceptance rule that we have used in the insertion algorithm.

### IV. EFFICIENCY

#### A. Wall-wall effective pair potential

To validate the present method, we first applied it to compute the depletion interaction due to non-adsorbing, self-avoiding polymers between hard walls. This system provides a convenient yet nontrivial test of our algorithm, as Bolhuis *et al.* [9] and Tuinier *et al.* [10] have calculated the depletion interaction of SAW polymers between hard walls using configurational bias MC, over a wide range of polymer densities. The depletion attraction can be computed by determining the

grand-partition function  $\Xi$ , at fixed chemical potential  $\mu$ . For each separation between two walls a thermodynamic integration relates the grand-partition function  $\Xi$ , to the average number of particles in the system  $\langle N(\mu') \rangle$ ,

$$k_B T \ln \Xi(\mu, d) = \int_{-\infty}^{\mu} \langle N(\mu') \rangle d\mu'. \quad (7)$$

The depletion interaction follows by subtracting the bulk contribution to the grand potential and the contribution due to two non-interacting surfaces. In what follows, we denote the radius of gyration of the polymers by  $R_G$ . The overlap concentration  $\rho^*$  will be defined as  $1/v_p$ , in which  $v_p = 4/3 \pi R_G^3$  is the effective volume of a single polymer coil. Systems with concentrations well below  $\rho^*$  are considered to be dilute. Here, we report results for three densities and compare the results with those reported in Refs. [9,10].

We carried out grand-canonical MC simulations for self-avoiding polymers of length  $l=100$ . The polymers were simulated on a cubic lattice between two hard walls. Several simulation were carried with different spacing between the walls. In the direction parallel to the walls, we employed

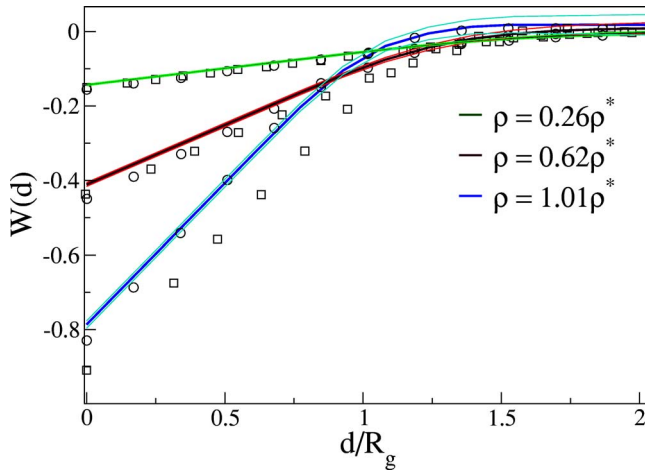


FIG. 1. (Color online) Depletion interaction for athermal, self-avoiding lattice polymers between unstructured hard walls. The strength of the depletion interaction is expressed in units  $k_B T / R_G^2$ . The three sets (lines) correspond to three different densities  $0.26\rho^*$ ,  $0.62\rho^*$ , and  $1.01\rho^*$ , where  $\rho^*$  denotes the overlap concentration (see, text). The parallel shadowed lines indicate the errorbars. The corresponding data points of Refs. [9,10] are indicated as squares and circles.

periodic boundary conditions. The lateral size of the periodic box was  $50 \times 50$  lattice sites. Hard-core repulsions were defined to exclude conformations where two monomers occupy the same lattice site. For the Monte Carlo moves we used the “wormhole method” of Houdayer [7]. The method described above was used for polymer insertion and deletion. We calculated the average number of particles as a function of chemical potential. We started from a very dilute regime (corresponding to  $\mu = -\infty$ ) to get a correct estimation of  $\Xi$ . When the surface separation is large,  $kT \ln \Xi$  contains only the bulk contribution (that can be computed for a system without walls) and the constant contribution due to two non-interacting walls,  $2\gamma_w A$ , where  $A$  is the surface area of the hard wall. Hence, by comparing  $kT \ln \Xi$  for a bulk system and a system with the same number of lattice sites, but enclosed between two hard walls, we immediately obtain  $\gamma_w$ . Figure 1 shows the results of these simulations for three different concentrations. Within the regime where scaling arguments are valid, the depth and range of the potential depend only on the radius of gyration and concentration. As expected, the depth of the potential increases with increasing polymer density. In view of the large difference between the results of Refs. [9,10], our results appear consistent with both (unfortunately, neither paper quotes error bars). Our data are closest to those of Ref. [10]. We note that, in order to reproduce the bulk densities of Refs. [9,10] for a chain with length 100 we assumed  $R_G \approx 6.476$  as was calculated by Nickel [11]. Our error estimates in Fig. 1 have been calculated by taking into account the statistical errors in integration, fitting and subtracting.

Compared to the CBMC method, MP has a higher insertion rate per MC trial move; in the above case, it is some 100 times higher. However, the CBMC method is much less time consuming. We performed the same simulation with the CBMC method to compare the efficiency and found the

CBMC to be about 5000 times faster than MP in the above case. With both methods higher densities can be simulated. For chains of length  $L=100$  densities up to  $3\rho^*$  are feasible. To conclude, with the MP method we can reproduce the earlier CBMC results. However, for the specific problem of nonadsorbing polymers between hard walls, CBMC is clearly the method of choice.

Although MP fails to bring an improvement for systems with only hard core interactions, it turns out to be more useful in problems with different kinds of interactions. MP is far more efficient in identifying rare configurations with very low energy (i.e., with large Boltzmann weight). A good example is a system of polymers with strongly interacting end groups. Such polymers can bind to each other or to specific binding sites on surfaces. A case in point is the binding of DNA chains with single-stranded end segments, to colloids coated with complementary single-stranded (ss) DNA. Such polymers can form bridges between colloids or form loops on single surfaces. The interactions between surfaces are the combination of bridging attraction, steric repulsion of the loops or dangling polymers, and depletion of the free linkers. In order to compute the effective interaction free energies between the surfaces, it is crucial, yet difficult, to sample well equilibrated systems. Here the advantage of the present moment-propagation scheme over CBMC becomes clear.

## B. Tethered polymers

In order to test the efficiency of MP on the above-mentioned class of problems, we performed simulations on systems with end-associating polymers between two walls. Apart from the end-group interactions, the system is the same as the one described in the previous section. Each polymer is considered as a SAW chain which in this case can attach to the surfaces with its terminal groups, due to a strong, short-ranged attraction. In what follows, we will consider the specific case that the two walls are identical. This implies that polymers can either form loops by adsorbing both their ends on one wall, or form bridges by attaching to both surfaces. In addition, the polymers may have one or two end groups unbound. The range of the binding interaction is set to one lattice spacing, meaning that the binding sites are placed next to the hard wall. The surface grafting density  $\rho_s$  measures the fraction of binding sites at each layer. The binding energy  $\epsilon_b$  is defined as the depth of the attractive potential. Other parameters such as the bulk density  $\rho$  and the separation between the hard walls affect the computational efficiency. Most of the existing methods fail to equilibrate systems at high densities. Also finding bridged conformations is increasingly difficult at higher densities, especially when the separation between the surfaces is large compared to  $R_g$  (because then the most favorable links are highly stretched).

Figure 2 shows a typical example of the difference in performance between CBMC and MP methods. The results shown in this figure correspond to a situation where the grafting density  $\rho_s=0.02$ , which corresponds to 50 sites per wall in our case. We chose a relatively large binding energy:  $\epsilon_b=10k_B T$ . Such large values are not unphysical: for in-

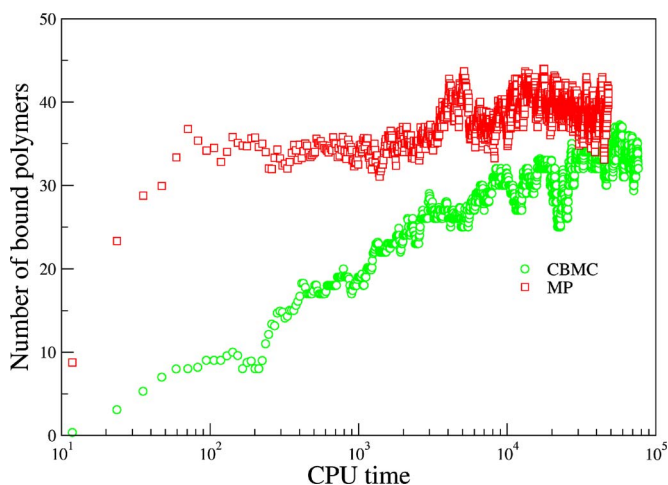


FIG. 2. (Color online) Rate of equilibration of the number of bound (bridge or loop) polymers between two walls as computed using the MP scheme (squares) and the CBMC scheme (circles). The horizontal axis indicates the required CPU time. The spacing between the two walls is 8 lattice units. The volume fraction of monomers is 0.23. The fraction of binding sites on the surface,  $\rho_s=0.02$ . The binding energy,  $\epsilon_b=10k_B T$ .

stance, the hybridization free energy with which DNA strands bind to ssDNA coated colloids is in this range. For instance, the hybridization of ssDNA of 14 bases is in the range of  $(25-30)k_B T$  [12]. In our simulation every chain has two interacting ends, i.e., the energy of a bound configuration is  $2\epsilon_b=20k_B T$ . The bulk monomer volume fraction,  $\rho_{mon}=0.23$ . As can be seen from the figure, the CPU time needed for equilibration is much less when using the MP method than with the CBMC method. In fact, the CBMC method seems to fail to equilibrate the system, even for the longest runs. We note that the two methods approach equilibrium in a very different way. Starting from very dilute initial conditions, the MP scheme first grows bound configurations. In most cases, these bound configurations reach their equilibrium value even faster than those that are free. The reason why the MP scheme favors configurations with higher Boltzmann weight in the selection process is that the Boltzmann-weighted numbers  $\omega'$  [see Eq. (1)] provide information about accessible configurations. By contrast, the CBMC method initially fills the system with dangling and free polymers. This makes it subsequently more difficult to reach the equilibrium density of bound configurations.

To check the efficiency of our method we performed simulations for three different grafting densities  $\rho_s=0.02, 0.2$ , and  $1.00$ , and different binding energies  $\epsilon_b/(k_B T)=5, 10$ . We also studied the system both in a narrow gap  $d=3$ , and at larger distances like  $d=8$ , and we tried different bulk densities.

On the basis of these simulations, we reach the following tentative conclusions: At high grafting densities the MP scheme is less useful. This comes about because in equilibrium all polymers will be bound. Then all configurations have the same energy and there is no need for a scheme (such as MP) that will identify rare configurations that have a much higher Boltzmann weight than most others. As one

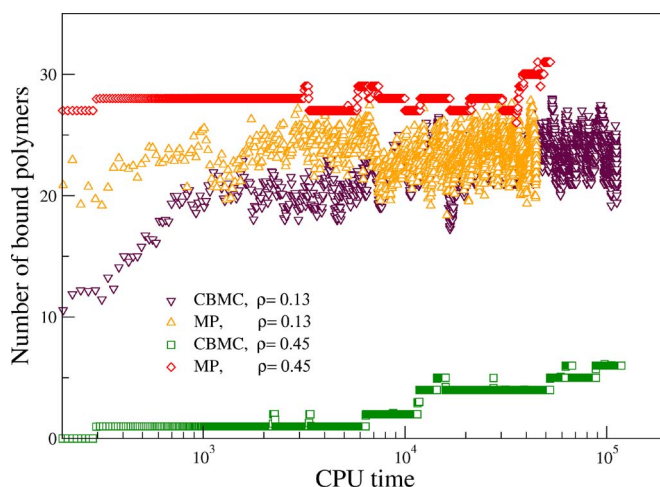


FIG. 3. (Color online) Density dependence of the equilibration rate of the MP and CBMC schemes. The figure shows the number of bound (bridge or loop) polymers between two walls as a function of CPU time. As in Fig. 2, the spacing between the two walls is 8 lattice units. The fraction of binding sites on the surface,  $\rho_s=0.02$  and the binding energy,  $\epsilon_b=10k_B T$ . Results are shown for a high monomer concentration (45%) and a low monomer concentration (13%). The inset shows the density dependence of the number of bound polymers.

might expect, both methods become inefficient at high densities and large wall-wall separations. However, the results show that increasing polymer density affects the CBMC method much more adversely than MP. We compared the two methods at low and high densities in Fig. 3. At high densities, the CBMC simulation fails to find bound chains, while MP is much closer to the equilibrated system. The MP method is therefore the method of choice in cases where there is a large heterogeneity in binding energies and in systems where the accessible volume per polymer is small. Both situations are relevant for the study of selective binding of biomolecules to specific substrates. Interestingly, the results shown in Figs. 2 and 3 suggest that the number of bound polymers is not a monotonic function of density. It first increases with increasing density and then decreases (see Fig. 3 inset). We can see this effect with the approach presented in this paper, but not with the CBMC method. Still, we should caution that, even with the MP method, it is difficult to obtain high statistical accuracy at high polymer densities.

## V. CONCLUSION

We presented a biased Monte Carlo method for lattice polymers based on the moment propagation scheme. The method uses nonreversible statistics as guiding weights to grow self-avoiding polymers. We showed that it is feasible to implement the MP scheme in such a way that detailed balance is satisfied. In order to test the efficiency of the MP method, we specifically applied it to two set of problems. First we computed the depletion interaction between two plates and compared results with existing data [9]. The results show that the MP scheme quantitatively reproduces the known behavior of this model system. However, the MP ap-

proach is less efficient than CBMC in this case. This situation is reversed in the case of telechelic polymers between two plates. We showed that, in particular in the case of highly heterogeneous surfaces, the MP method is more efficient than the CBMC method. Moreover, the relative advantage of MP is more pronounced at high volume fractions.

The MP scheme can be applied to any regular lattice. However, the efficiency of the method is sensitive to the nature of the interactions between monomers. In general the MP method is expected to be more efficient than alternative schemes when searching for rare configurations with low en-

ergy. Many problems involving the specific binding of a biomolecule (be it a protein or a ssDNA segment) to a substrate are of this nature.

#### ACKNOWLEDGMENTS

The work of the FOM Institute is part of the research program of FOM and is made possible by financial support from the Netherlands organization for Scientific Research (NWO). The authors are grateful to A. Arnold and H. Tepper for their comments.

- 
- [1] K. Kremer and K. Binder, *Comput. Phys. Rep.* **7**, 259 (1988).
  - [2] K. Binder *Monte Carlo and Molecular Dynamic Simulations in Polymer Science* (Oxford University Press, New York 1995).
  - [3] A. D. Sokal, in *Monte Carlo and Molecular Dynamics Simulations in Polymer Science* (Oxford University Press, New York, 1995), pp. 47–124.
  - [4] D. Frenkel and B. Smith, *Understanding Molecular Simulations* (Academic Press, San Diego, 1995).
  - [5] N. C. Karayiannis, V. G. Mavrantzas, and D. N. Theodorou, *Phys. Rev. Lett.* **88**, 105503 (2002).
  - [6] Q. L. Yan and J. J. De Pablo, *J. Chem. Phys.* **111**, 9509 (1999).
  - [7] J. Houdayer, *J. Chem. Phys.* **116**, 1783 (2002).
  - [8] G. C. A. M. Mooij and D. Frenkel, *Mol. Phys.* **74**, 41 (1991).
  - [9] P. G. Bolhuis, A. A. Louis, and J. P. Hansen, *J. Chem. Phys.* **114**, 4296 (2001).
  - [10] R. Tuinier, D. G. A. L. Aarts, H. H. Wensink, and H. N. W. Lekkerkerker, *Phys. Chem. Chem. Phys.* **5**, 3707 (2003).
  - [11] B. G. Nickel, *Macromolecules* **24**, 1358 (1991).
  - [12] P. L. Biancaniello, A. J. Kim, and J. C. Crocker, *Phys. Rev. Lett.* **94**, 058302 (2005).